International Journal of Computer Information Systems and Industrial Management Applications.
ISSN 2150-7988 Volume 4 (2012) pp. 411–419

Useful Noise Effect for Nonlinear PDE Based Restoration of Scalar Images

Aymeric Histace[1] **and David Rousseau**[2]

[1]Université de Cergy-Pontoise, ETIS ;
CNRS UMR8051; ENSEA ; France
aymeric.histace@u-cergy.fr

[2]Université de Lyon, CREATIS ;
CNRS UMR5220 ; Inserm U1044 ; INSA-Lyon ; Université Lyon 1, France.
david.rousseau@univ-lyon1.fr

Abstract: **It is progressively realized that noise can play a constructive role in the domain of nonlinear information processing. This phenomenon, also known as stochastic resonance (SR) effect, has experienced large varieties of extensions with variations concerning the type of noise, the type of information carrying signal or the type of nonlinear system interacting with the signal-noise mixture. In this article, we propose an interpretation for the mechanism of noise-enhanced image restoration with nonlinear PDE (Partial Differential Equation) recently demonstrated in literature. More precisely, a link is established between the action of noise in a nonlinear Perona–Malik anisotropic diffusion and stochastic resonance in memoryless nonlinear systems for 1-D signals. For illustration some preliminary results are presented on classical "cameraman" image and the inner of SR mechanism is theoretically and practically studied using a simple set of parameters regarding the PDE used and the modeling of boundaries within images.**

Keywords: Stochastic resonance, anisotropic diffusion, image restoration, nonlinear image processing.

I. Introduction

It is progressively realized that noise can play a constructive role in the domain of nonlinear information processing. The starting point of the investigation of such useful noise effect has been the study of stochastic resonance [1, 2, 3]. Originally introduced to describe the mechanism of a constructive action of a white Gaussian noise in the transmission of a sinusoid by a nonlinear dynamic system governed by a double well potential [4, 5], the phenomenon of stochastic resonance has experienced large varieties of extensions with variations concerning the type of noise, the type of information carrying signal or the type of nonlinear system interacting with the signal-noise mixture (see [6] for a review in physics, [7] for an overview in electrical engineering and [8, 9] for the domain of signal processing). All these extensions of the original setup preserve the possibility of improving the processing of a signal by means of an increase in the level of the noise coupled to this signal. New forms of useful-noise effect, related to stochastic resonance or not, continue to be demonstrated [10, 11, 12, 13, 14, 15, 16]. A current domain of interest is the study of nontrivial transposition of stochastic resonance to image processing [17, 18, 19, 20] and more particularly to nonlinear image restoration.
We discuss here the possibility to enhance nonlinear PDE image restoration with a controlled useful injection of noise. In previous communications , we have proposed to tackle this standard restoration task with a stochastic variant of Perona-Malik's process.
The report is organized as follow: we first recall the global framework of stochastic resonance and introduce the stochastic anisotropic diffusion equation originally proposed in [21, 22]. We then study a simplified version of this equation stochastic diffusion equation preserving the essential properties of the former historical equation proposed in [23]. Therefrom, we establish a formal analogy between the mechanism of useful-noise effect in image anisotropic diffusion and the mechanism of stochastic resonance in static non-linearity with additive signal–noise mixture in monodimensional signals.

II. Global scheme of stochastic resonance

From an informational point of view [8], stochastic resonance (SR) can be described with the general scheme of Fig. 1 which involves four essential elements: (i) an information-carrying or coherent signal s: it can be deterministic, periodic or non, or random; (ii) a noise η, whose statistical properties can be of various kinds (white or colored, Gaussian or non,...); (iii) a process, which generally is nonlinear, receiving s and η as inputs under the influence of which it produces the output signal y; (iv) a measure of performance, which quantifies the input–output information transmission (it may be a signal-to-noise ratio, a correlation coefficient, a Shannon mutual information, ...). By contrast with the informational scheme of Shannon, the noise in Fig. 1 is considered as an input with a tunable level. A useful-noise effect occurs when the input–output information transmission, assessed with the chosen measure of performance, is

enhanced from an increase of the level of the noise.

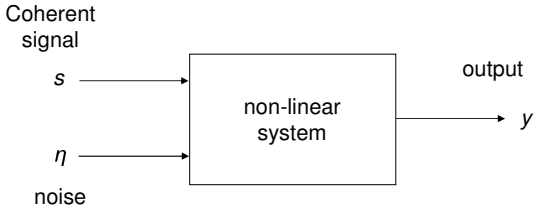

Figure. 1: Stochastic resonance consists in the possibility of increasing the transmission of information between the input signal s and the output signal y by means of an increase of the level of the noise η.

Historically, the developments of SR have proceeded through variations and extensions over these four basic elements. From the origin, SR studies have concentrated on a periodic coherent signal s, transmitted by nonlinear systems of a dynamic and bistable type. This form of SR now appears simply as a special form of useful-noise effect. This primary form of SR will not be entirely described in this article but a complete description can be found in [4, 5] for instance. For illustration, we propose to illustrate phenomenon of SR in the framework of image transmission as it was formerly proposed in [8]. This example has the advantage of its simplicity which makes both theoretical and experimental analysis possible. Leaning again on the general scheme of SR phenomenon, author considers this time that the coherent information-carrying signal s is a bidimensional image where the pixels are indexed by integer coordinates (i, j) and have intensity $s(i, j)$. For a simple illustration, a binary image with $s(i, j) \in \{0, 1\}$ is considered for experiment. A noise $\eta(i, j)$, statistically independent of $s(i, j)$, linearly corrupts each pixel of image $s(i, j)$. The noise values are independent from pixel to pixel, and are identically distributed with the cumulative distribution function $F_\eta(u) = Pr\{\eta(i, j) \leq u\}$. A nonlinear detector, that it is taken as a simple hard limiter with threshold θ, receives the sum $s(i, j) + \eta(i, j)$ and produces the output image $y(i, j)$ according to:

$$\begin{array}{lll} \text{If } s(i,j)+\eta(i,j) > \theta & \text{then} & y(i,j) = 1, \\ & \text{else} & y(i,j) = 0. \end{array} \qquad (1)$$

When the intensity of the input image $s(i, j)$ is low relative to the threshold θ of the detector, i.e. when $\theta > 1$, then $s(i, j)$ (in the absence of noise) remains undetected as the output image $y(i, j)$ remains a dark image. Addition of the noise $\eta(i, j)$ will then allow a cooperation between the intensities of images $s(i, j)$ and $\eta(i, j)$ to overcome the detection threshold. The result of this cooperative effect can be visually appreciated on Fig. 2, where an optimal nonzero noise level maximizes the visual perception.
To quantitatively characterize the effect visually perceived in Fig. 2, an appropriate quantitative measure of the similarity between input image $s(i, j)$ and output image $y(i, j)$, is provided by the normalized cross-covariance defined in [24] and given by:

$$C_{sy} = \frac{\langle (s - \langle s \rangle)(y - \langle y \rangle) \rangle}{\sqrt{\langle (s - \langle s \rangle)^2 \rangle \langle (y - \langle y \rangle)^2 \rangle}} , \qquad (2)$$

Figure. 2: The image $y(i, j)$ at the output of the detector of Eq. (1) with threshold $\theta = 1.2$, when $\eta(i, j)$ is a zero-mean Gaussian noise with rms amplitude 0.1 (left), 0.5 (center) and 2 (right).

where $\langle . \rangle$ denotes an average over the images.
C_{sy} can be experimentally evaluated through pixels counting on images similar to those of Fig. 2. Also, for the simple transmission system of Eq. (1), C_{sy} can receive explicit theoretical expressions, as a function of $p_1 = Prs(i, j) = 1$ the probabilty of a pixel at 1 in the binary input image $s(i, j)$, and as a function of the properties of the noise conveyed by $F_\eta(u)$ as mentioned in [24].
Considering the above scenario, Fig. 3 shows variations of C_{sy} function of rms amplitude of the input noise η.

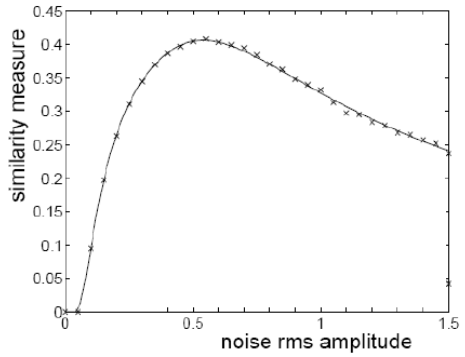

Figure. 3: Input-output cross-covariance of Eq. (2) between input image $s(i, j)$ and output image $y(i, j)$, as a function of the rms amplitude of the noise $\eta(i, j)$ chosen zero-mean Gaussian. The crosses are experimental evaluations through pixels counting on images, the solid lines are the theoretical predictions ($p_1 = 0.6$) calculated by authors [8].

As one can see on Fig. 3, measure of cross-covariance as defined Eq. (2) identify a maximum efficacy in image transmission for an optimal nonzero noise level. This simple example is interpreted here as the first formalized instance of SR for aperiodic bidimensionnal input signal s (even if it is not clearly an image processing application).
We are now going to show that this kind of approach can be successfully transposed in the framework of nonlinear PDE based image restoration approach.

III. A stochastic variant of the Perona–Malik process for image restoration

A. *Framework*

In the particular field of image restoration, nonlinear or anisotropic regularization PDE's are of primary interest. The benefit of PDE-based regularization methods lies in their

ability to smooth data in a nonlinear way, allowing the preservation of important image features (contours, corners or other discontinuities). In the particular domain of scalar image restoration, the introduction of the Perona–Malik process [23] as triggered a large interest [25, 26, 27, 28, 29, 30, 31, 32, 33, 34, 35, 36] for a selected list of papers.
In the original Perona–Malik process the observable noisy image ψ_0 is restored by considering the solution of the partial differential equation given by

$$\frac{\partial \psi}{\partial t} = div(g(\|\nabla\psi\|)\nabla\psi), \qquad \psi(x,y,t=0) = \psi_0 \ , \quad (3)$$

where the anisotropy of this diffusion process is governed by $g(\cdot)$ a nonlinear decreasing function of the norm of the gradient $\nabla\psi$. In this study, we consider a variant of the standard Perona–Malik's process of Eq. (3) introduced in [21], where the anisotropic diffusion process, given by

$$\frac{\partial \psi}{\partial t} = div(g_\eta(\|\nabla\psi\|)\nabla\psi) \ , \quad (4)$$

which is of a form similar to Eq. (3) except for the nonlinear function $g_\eta(\cdot)$ which is given by

$$g_\eta(u) = g(u + \eta(x,y)) \ , \quad (5)$$

where η is a noise assumed independent and identically distributed with probability density function $f_\eta(u)$ and rms amplitude σ_η. The noise η, which is distinct from the native noise component ξ to be removed, is a purposely added noise applied to influence the operation of $g(\cdot)$. In [21], we have shown that the injection of a Gaussian noise in Eq. (5) can improve the restoration process by comparison with standard Perona-Malik process of Eq. (3) when the native noise component ξ is a Gaussian, impulsive or multiplicative noise and with $g(\cdot)$ given by

$$g(u) = e^{-\frac{\|u\|^2}{k^2}} \ . \quad (6)$$

In this expression, parameter k can be seen as a soft threshold controlling the decrease of $g(\cdot)$ and the amplitude of the gradients to be preserved from the diffusion process. Our previous works [21] and [22] have shown, as a proof of feasability, that an injection of a non zero amount of noise could help the restoration process when the threshold k is ill-positioned.

B. Preliminary results

For illustration, the image "cameraman" (see image (d) in Fig. 4), is chosen as reference for the original image ψ_{ori}. Noisy versions of this original image are presented as the observable images ψ_0 of our restoration task in Fig. 4 for various image–noise coupling.
A visual appreciation of the performance of the stochastic version of Perona–Malik process of Eq. (4) and the original Perona–Malik process of Eq. (3) is shown in Fig. 5.
The images restored by the stochastic process appear to be of better visual interest than those obtained with the classical Perona–Malik process for all the three types of noise component tested. This is especially visible, in Fig. 5, in areas of the "cameraman" image characterized by small gradients (face, buildings in the background, or textured area like grass) which are preserved from the diffusion process and

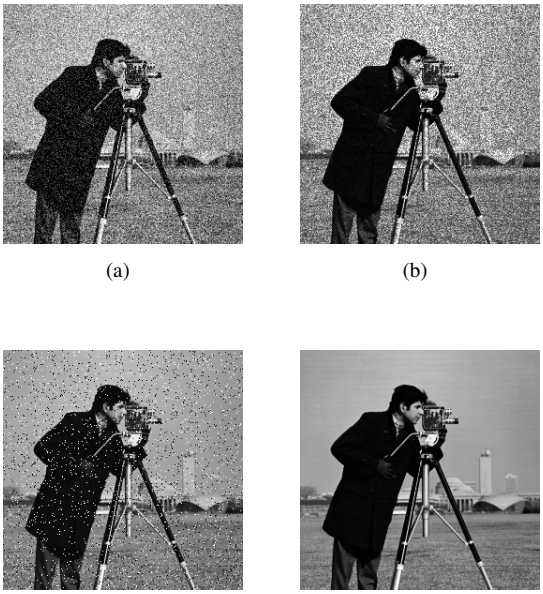

Figure. 4: The original image ψ_{ori} cameraman (d) corrupted by three different native noises ξ: (a) additive zero-mean Gaussian noise with $\psi_0 = \psi_{ori} + \xi$, (b) multiplicative Gaussian noise of mean unity with $\psi_0 = \psi_{ori} + \xi.\psi_{ori}$, (c) impulsive noise.The rms amplitude of these noises are separately adjusted in order to have each of the images (a,b,c) characterized by the same normalized crosscovariance (given in Eq. (7)) with the original image equal to 0.87.

better restored with the presented stochastic approach than with the classical Perona–Malik process.
A quantitative analysis is presented in Fig. 6 where the number of iteration n of the diffusion processes is fixed. For our purpose, the normalized crosscovariance is adapted to the framework of image restoration by iterative process considering the following equation:

$$C_{\psi_{ori}\psi(t_n)} = \frac{\langle(\psi_{ori} - \langle\psi_{ori}\rangle)(\psi(t_n) - \langle\psi(t_n)\rangle)\rangle}{\sqrt{\langle(\psi_{ori} - \langle\psi_{ori}\rangle)^2\rangle\langle(\psi(t_n) - \langle\psi(t_n)\rangle)^2\rangle}} \ , \quad (7)$$

with $\langle..\rangle$ a spatial average, $\psi(t_n)$ the different restored steps calculated with Eq. (4), for (i) g_{eff} and (ii) g_η, at discrete instants $t_n = n\tau$.
Variation of this similarity measure is then presented as a function of the rms amplitude σ_η of the Gaussian noise purposely injected. As visible in Fig. 6, the normalized crosscovariance of Eq. (7) experiences, for all the 3 tested noise components, a nonmonotonic evolution and culminates at a maximum for an optimal nonzero level of the injected Gaussian noise. These results are in good accordance with the direct visual inspection of the images and demonstrate the possibility of improving the performance of the Perona–Malik process by injecting a non zero amount of the noise η with various image–noise coupling.
We now propose to investigate the inner mechanism of the useful-noise effect shown in [21, 22]. To this purpose, we propose to simplify the nonlinear function $g(\cdot)$. The diffusive function of Eq. (6) was chosen in [21] because it corresponds

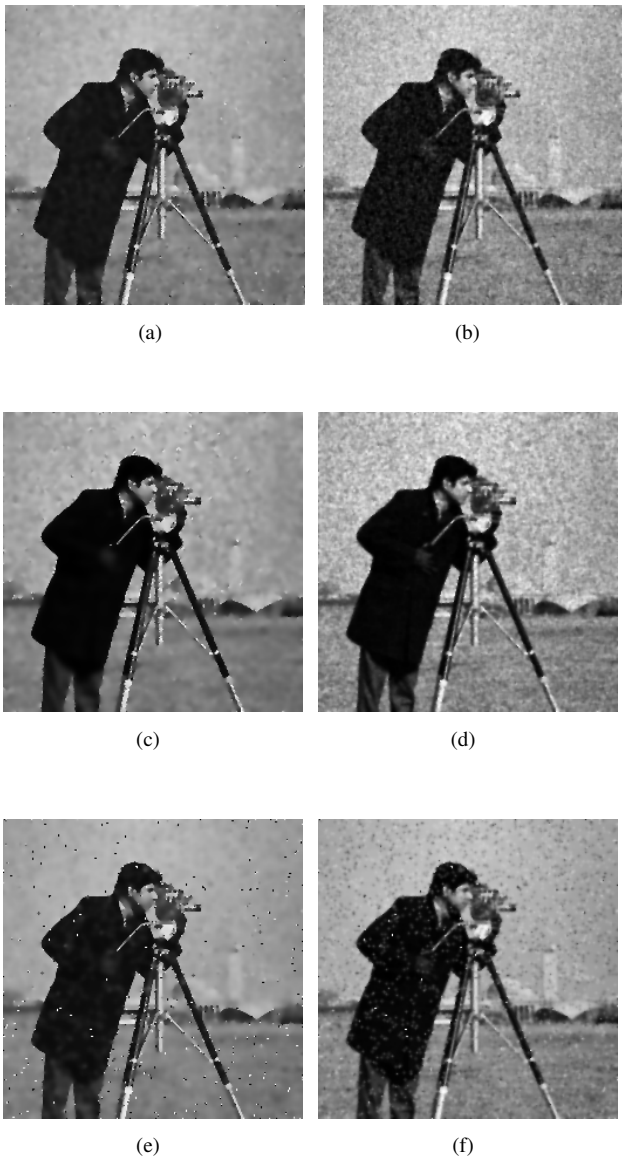

(a) (b)

(c) (d)

(e) (f)

Figure. 5: Visual comparison of the performance of the original restoration Perona–Malik process and the corresponding stochastic version. The left column shows the results obtained with usual Perona-Malik restoration process and the right column with our stochastic version of the Perona–Malik process. Each image is obtained with the iteration number n corresponding to the highest value of the normalized crosscovariance. The top (a,b), middle (c,d) and bottom (e,f) lines are respectively standing for the additive, multiplicative and impulsive noise component described in Fig. 4.

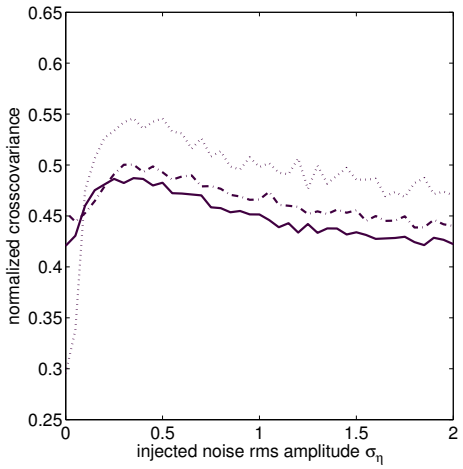

Figure. 6: Normalized crosscovariance of Eq. (7) as a function of the rms amplitude σ_η of the Gaussian noise η purposely injected with the number of iteration n which is fixed to $n = 15$. Solid, dash-dotted and dotted lines are respectively standing for the additive, multiplicative and impulsive noise components described in Fig. 4

to the historical function proposed in [23]. This choice nevertheless presents some drawbacks for the complete understanding of the useful-noise effect since the presence in the analytical definition of $g(\cdot)$ function of a L_2 norm of the purposely noised gradient of the image leads to an offset shifting that makes the interpretation of the impact of the noise uneasy.

C. A simple set of parameters

In this article, we choose to simplify the shape of $g(\cdot)$ into a hard threshold non-linearity given by

$$g(s) = \begin{cases} 1 \text{ if } s \geq k \\ 0 \text{ if } s < k \end{cases} , \tag{8}$$

where parameter k is now a hard threshold. This function integrates a hard non-linearity in order to set in a binary way the diffusion threshold. Moreover, this non-linearity is only function of the norm of the gradient in order to only emphasis the effect of the purposely injection of noise and to avoid the shifting effect described above. One can note that despite this methodological choice regarding $g(\cdot)$ function, this latter is just a simplified version of the former function proposed in [23] and still embed the fundamental elements of the classical anisotropic diffusion.

For illustration, the data to be restored is also chosen in its most simplest form. We consider a monodimmensional signal ψ_{ori} taken as a unit step function modeling an edge within a noisy image. ψ_0 will denote the noisy version of ψ_{ori}. The goal is now to restore the noisy step version without altering the hard discontinuity of ψ_{ori}. More, we want to show that injection of noise within the restoration process can lead to overpass the classical weak point of Perona-Malik process: a lack of robustness regarding k parameter.

Parameter k of Eq. (8) plays a very important role in the study as far as little variations of its value can lead to completely different results of restoration. For instance, let us consider ψ_{ori} as defined Fig. 7.

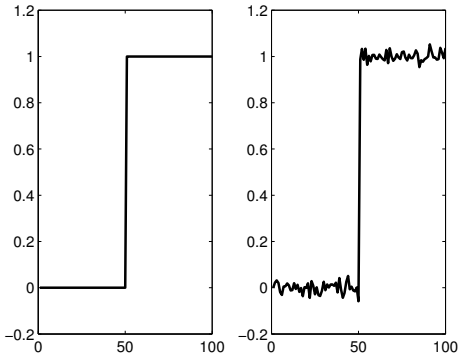

Figure. 7: Illustration of the monodimensional function used for the study. On the left, the original ψ_{ori} function. On the right, the corrupted version ψ_0 (ξ is chosen gaussian).

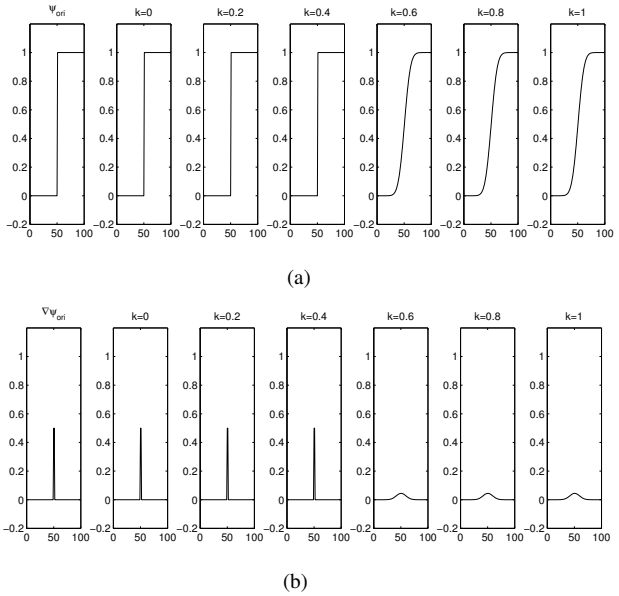

(a)

(b)

Figure. 8: Illustration of the lack of robustness of classical Perona-Malik's process of Eq. (3) regarding parameter k. $g(.)$ is given by Eq. (8), iteration number n is fixed to 200, and time step τ to 0.2. (a) shows for each value of k the obtained diffused step, and (b) the corresponding gradient function. This Figure shows that the possibility to remove noise without smoothing the discontinuity of ψ_0 strongly depend on the value of k.

To apply classical Perona-Malik process of Eq. (3) to ψ_{ori}, Eq. (3) is discretized with a time step τ such as $t_n = n\tau$ where n is the number of iterations in the process and t_n the corresponding scale.

Fig. 8 shows that the classical Perona-Malik process of Eq. (3) with $g(\cdot)$ given by Eq. (8) presents a lack of robustness regarding parameter k as far as for different values of this parameter ($k \in \{0; 0.2; 0.4; 0.6; 0.8; 1\}$) final result of each corresponding diffusion process is quite different.

More precisely, one can notice in Fig. (8) that for $k < 0.5$ ψ_{ori} is not altered by the diffusion process of Eq. (3), whereas for $k > 0.5$ ψ_{ori} is diffused as far as a smoothing is introduced which tends to attenuate the maximum value of the corresponding gradient and to spread its width along x-axis. This can be interpreted as an alteration of boundaries within images for a bad tuning of k.

This drawback is all the more embarrassing as the smoothing discrimination between noise and boundaries also depends on the value of k as one can notice on Fig. 8.

In [21] we have shown that the stochastic variant of Perona-Malik process of Eq. (4) has a stronger robustness toward the tuning of parameter k. We provide an interpretation of the mechanism for this useful-noise effect.

IV. Stochastic restoration: theoretical study

A. Preliminary calculations

The non-linearity of Eq. (4) can be classified as a static or memoryless non-linearity. Possibility of useful-noise effect in static non-linearity has been intensively studied (see [9] for a review). The action of the additive noise $\eta(x, y)$ can be understood as a shaping by noise of the input–output characteristic which on average becomes equivalent to

$$g_{eff}(s) = E[g(s + \eta(x, y))] = \int_{-\infty}^{+\infty} g(u) f_\eta(u - s) du \ , \tag{9}$$

with $f_\eta(u)$ the probability density function of the purposely injected noise η. In the case of the hard quantizer of Eq. (8) with threshold k, Eq. (9) becomes

$$g_{eff}(s) = F_\eta(k - s) \ , \tag{10}$$

where F_η is the cumulative distribution function of the probability density function of $f_\eta(u)$. If we consider the case where $f_\eta(u)$ is uniform we have

$$g_{eff}(s) = \begin{cases} 0 \text{ for } k - s \leq -\sqrt{3}\sigma_\eta \\ \frac{1}{2}\left(1 + \frac{k-s}{\sqrt{3}\sigma_\eta}\right) \text{ for } |k - s| < \sqrt{3}\sigma_\eta \\ 1 \text{ for } k - s \geq \sqrt{3}\sigma_\eta \end{cases} . \tag{11}$$

$g_{eff}(\cdot)$ function corresponds to the average theoretical equivalent characteristic of $g_\eta(\cdot)$ in presence of a purposely added noise with standard deviation σ_η.

B. Experiment

We now propose to compare the behavior of the numerical diffusion process of Eqs. (5) and (8) with the equivalent theoretical input–output characteristic of Eq. (9). We choose

the noisy step ψ_0 of Fig. 9.(a), and we assess the efficacy of the restoration process with the normalized cross-covariance as previously defined (Eq. 7).
As noticeable in Figs. 9.(b) and 9.(c), restoration results are in good accordance between numerical simulation and theoretical relation (standard deviation of ξ noise is set to 0.05 for illustration).

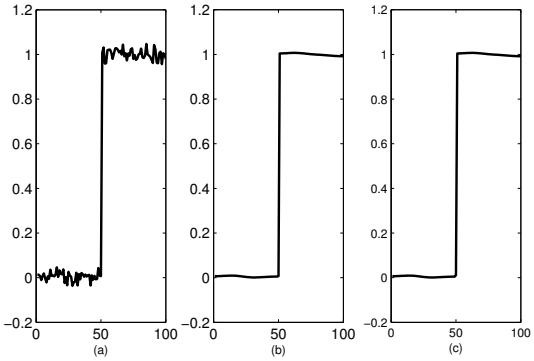

Figure. 9: Comparison between the numerical implementation of the stochastic diffusion process (Eqs. (5) and (8) and the theoretical one (Eq. (9)) on noisy step ψ_0.ξ noise is gaussian of standard deviation fixed to 0.05. iteration number n is fixed to 150. (a) ψ_0, (b) noise-enhanced diffusion proces (c) diffusion process with $g(\cdot) = g_{eff}(\cdot)$.

This agreement is also valid in Fig. 10 which shows ave age evolution of normalized cross-covariance (Eq. (7)) i terms of iteration number n calculated for 1000 diffusic processes.

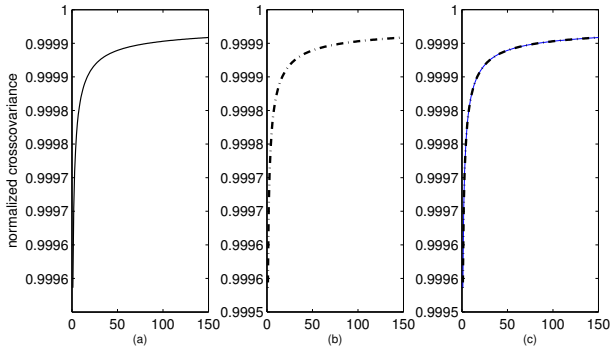

Figure. 10: Comparison of evolution of normalized cross-covariance for 1000 diffusion processes (Eq. (7) between the numerical implementation stochastic diffusion process (Eqs. (5) and (8) and theoretical one (Eq. (9)) on noisy step ψ_0. n is fixed to 150. (a) noise-enhanced diffusion process, (b) diffusion process with $g(\cdot) = g_{eff}(\cdot)$, (c) superposition of both. One can notice that the scale for normalized crosscovariance is very tiny: this can be easily explained by the fact that even corrupted, the noisy version of the step function remains characterized by a high value of this parameter. Global variations still remain of primary importance and must be only considered for this study.

Fig. 10.(c) shows again a perfect matching between both average evolution curves.
These results establish the link between the useful-noise effect shown in [21] and the mechanism at work in static nonlinear systems as described in [9].

V. Study of the Stochastic Resonance effect

In order to further study the influence of an injection of noise in classical Perona-Malik process, we consider in this section that k (Eq. (8)) is badly tuned (i.e. $k > 0.5$).
Considering the stochastic version of Perona-Malik process (Eq. (4)) with $g(\cdot)$ given by Eq. (8), the purposely injected noise η is a zero-mean Gaussian noise characterized by a tunable rms amplitude σ_η. For a visual appreciation of the noise-enhanced process, we consider the noisy step ψ_0 of Fig. 7 and k is set to 0.6, which corresponds to a badly tuned value regarding Fig. 8. In these conditions, as shown in Fig. 11.(b), Perona-Malik process fails in denoising ψ_0 without altering its integrity. If we now consider the stochastic Perona-Malik process of Eq. (4) with same parametrization of k, addition of noise η acts as a random resetting of parameter k, and, as shown in Fig. 11.(c), sometimes makes the preservation of the discontinuity of ψ_0 possible whereas k was badly tuned. It is important to notice, that this positive effect does not occur systematically, because of the random nature of the noise η.

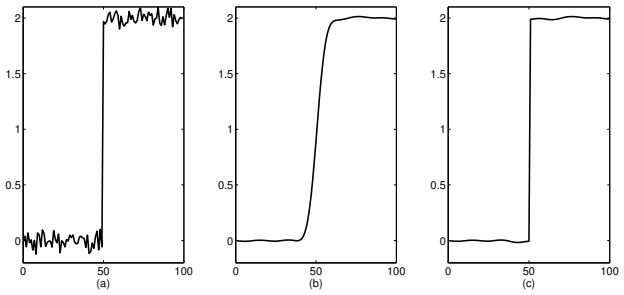

Figure. 11: (a) Noisy step $\psi_0 = \psi_{ori} + \xi$ (rms amplitude of ξ is fixed to 0.05), (b) Perona-Malik restoration of ψ_0 ($n = 50$), (c) Stochastic Perona-Malik restoration of ψ_0 ($n = 50$ and $\sigma_\eta = 0.3$. For (b) and (c), k is fixed to 0.6 (badly tuned). Injection of η noise makes possible to obtain a better restoration of the noisy step regarding the fact that noise is suppressed and step discontinuity is preserved.

Although the positive effect of injection of η noise is not systematic, this clearly demonstrates that an increase of the robustness of classical Perona-Malik process regarding parameter k is possible with the function $g_\eta(\cdot)$ proposed. Concerning the optimal amount of noise η to inject and the possibility to estimate the probability to have an averaged positive effect, we propose to quantitatively characterize the noise-enhanced effect shown Fig. 11 in the following way. We compute the percentage of well-restored steps (no alteration of the discontinuity) among a large number N of restoration attempts and for different values of σ_η, k being set up to a non optimal value. This ratio can be interpreted as a measure of the gain of robustness compare to the classical Perona-Malik process of Eq. (3) toward threshold k. Fig. 13 shows the evolution of the percentage of well restored steps for $k = 0.6$.
One can notice in Fig. 13 that the variations of the ratio of well restored steps is typical of the existence of a stochastic

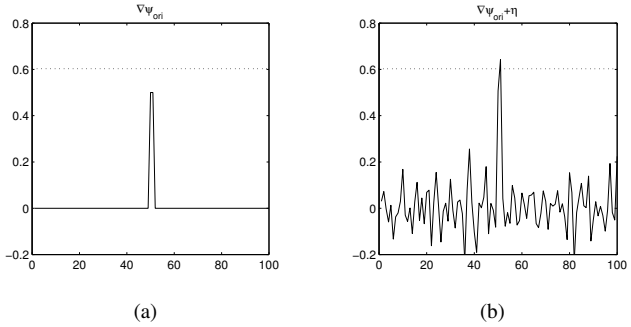

Figure. 12: (a) Solid line stands for variations of $\nabla\psi_{ori}$. Maximum value (0.5) is reached at the discontinuity of the studied step. Dotted line represents hard threshold k (fixed to 0.6 and considered as badly tuned) leading the diffusion process (Eq. (8)). (b) Solid line stands for variations of $\nabla\psi_{ori} + \eta$ (η is chosen gaussian) and dotted line still represents k-threshold. As one can notice in (b), sometimes the purposely injected noise η makes it possible to cross k-threshold, that is to say to locally tuned diffusion process in order to increase its robustness regarding k.

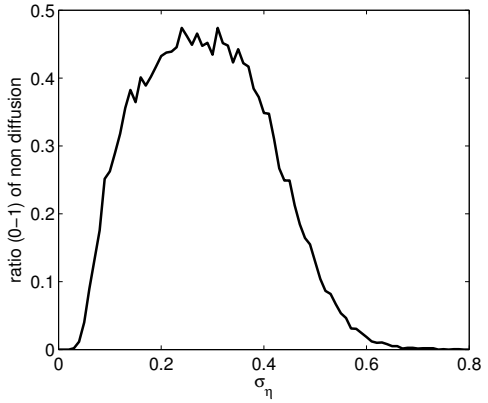

Figure. 13: Variation of the ratio of well restored steps (no alteration of the discontinuity) thanks to the purposely injection of η (Eq. (4)) function of rms amplitude σ_η. k is fixed to 0.6 and N, the total amount of restoration attempts, to 1000.

resonance effect related to a static ity where a maximum of the measure of performance is reached for a non zero amount of injected noise. Same experiments can be made for other badly-tuned values of k. Results are presented Fig. 14.

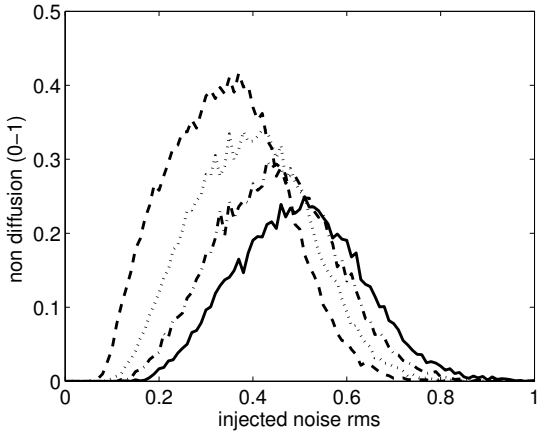

Figure. 14: Ratio of non-diffused steps function of rms amplitude σ_η. N is fixed to 1000. Dashed line stands for $k = 0.65$, dotted one for $k = 0.7$, dash-dotted one for $k = 0.75$ and solid one for $k = 0.8$. For each value of k, same stochastic effect as before (Fig. 13) can be observed : the non-diffusion ratio is maximum for a non zero amount of purposely injected noise.

As visible in Fig. 14, even if the maximum value of the ratio decreases, the useful-noise effect can be observed. This decrease can be easily explained by the fact the farer parameter k is from 0.5, the more important is the necessary amount of noise to inject to finally make an interesting retuning of k. As a consequence positive effect of purposely injected noise η is less important and presents a maximum for a value of σ_η also increasing (which can also be noticed on Fig. 14). Moreover, that type of curves also makes possible an evaluation of the optimal amount of noise to add regarding k values. For instance, it appears that for $k = 0.6$ (Fig. 13), a maximum probability of 46% of non diffusion of the discontinuity of ψ_{ori} can be reached for $\sigma_\eta = 0.3$ thanks to the stochastic Perona-Malik process.

VI. Conclusion

In this report, we have established a link between noised-enhanced anisotropic diffusion and stochastic resonance in static nonlinearities. This shows the way to non trivial transposition of stochastic resonance effect previously dedicated to monodimensional signal to images. Further investigations in the continuity of this report could deal with extensions to more complex nonlinear partial differential equation of the literature.

More precisely, in some recent publications ([14, 36]) dealing with diffusion processes for image restoration, particular nonlinear anisotropic PDE, integrating a double-well potential function of the form $f(\psi) = \psi(\psi - a)(\psi - 1)$, have been proposed. One of the obtained PDE [14] is an extension of the Fisher equation, derived from the Perona–Malik process, and given by

$$\frac{\partial \psi}{\partial t} = div(g(\|\nabla \psi\|)\nabla \psi) + f(\psi)\,. \qquad (12)$$

Such an equation has proved to be efficient for image enhancement. Nevertheless, sharpness preservation of the edge profiles remains a real challenge.

Moreover, Eq. (13) can be related to the evolution equation of dynamic systems as described in [8] for instance, for which SR phenomenon have been clearly identified, a complete theoretical and practical study of those type of PDE could be of real interest for image restoration. For such a study, the considered image restoration PDE could be of the form

$$\frac{\partial \psi}{\partial t} = div(g(\|\nabla \psi\|)\nabla \psi) + f(\psi) + \eta(x,y)\,. \qquad (13)$$

Establishment of a link between Fisher equation and stochastic resonance in dynamic nonlinearities could be of real interest to propose original restoration processes based on SR PDE and would extend the study proposed in this article but restricted to static nonlinearities.

References

[1] R. Benzi, A. Sutera, and A. Vulpiani, "The mechanism of stochastic resonance," *Journal of Physics A*, vol. 14, pp. L453–L458, 1981.

[2] R. Benzi, G. Parisi, A. Sutera, and A. Vulpiani, "Stochastic resonance in climatic changes," *Tellus*, vol. 34, pp. 10–16, 1982.

[3] K. Wiesenfeld and F. Moss, "Stochastic resonance and the benefits of noise: From ice ages to crayfish and SQUIDs," *Nature*, vol. 373, pp. 33–36, 1995.

[4] L. Gammaitoni, F. Marchesoni, E. Menichella-Saetta, and S. Santucci, "Stochastic resonance in bistable systems," *Physical Review Letters*, vol. 62, pp. 349–352, 1989.

[5] B. McNamara and K. Wiesenfeld, "Theory of stochastic resonance," *Physical Review A*, vol. 39, pp. 4854–4869, 1989.

[6] L. Gammaitoni, P. Hangi, P. Jung, and F. Marchesoni, "Stochastic resonance," *Reviews of Modern Physics*, vol. 70, pp. 223–287, 1998.

[7] G. Harmer, B. Davis, and D. Abott, "A review of stochastic resonance: Circuits and measurement," *IEEE Transactions on Instrumentation and Measurement*, vol. 51, pp. 299–309, 2002.

[8] F. Chapeau-Blondeau, *Noise, Oscillators and Algebraic Randomness- From Noise in Communication Systems to Number Theory*, ser. Lecture Notes in Physics. Springer (Berlin), 2000, vol. 550, ch. Stochastic resonance and the benefit of noise in nonlinear systems, pp. 137–155.

[9] F. Chapeau-Blondeau and D. Rousseau, "Noise improvements in stochastic resonance: From signal amplification to optimal detection," *Fluctuation and noise letters*, vol. 2, pp. 221–233, 2002.

[10] Q. Ye, H. Huang, X. He, and C. Zhang, "A sr-based radon transform to extract weak lines from noise images," in *Proceedings of ICIP*, vol. 1, no. 1, 2003, pp. 849–852.

[11] Q. Ye, H. Huang, and C. Zhang, "Image enhancement using stochastic resonance [sonar image processing applications," in *Proceedings of ICIP*, vol. 1, 2004, pp. 263–266.

[12] S. Blanchard, D. Rousseau, D. Gindre, and F. Chapeau-Blondeau, "Benefits from a speckle noise family on a coherent imaging transmission." *Optics Communications*, vol. 281, pp. 4173–4179, 2008.

[13] S. Morfu, P. Marquié, B. Nofiélé, and D. Ginhac, "Nonlinear systems for image processing," *Advances in imaging and electron. physics*, 2008.

[14] S. Morfu, "On some applications of diffusion processes for image processing," *Physics Letters A*, vol. 373, pp. 2438–2444, 2009.

[15] S. R. V.P. and P. Kumar Roy, "Magnetic resonance image enhancement using stochastic resonance in fourier domain," *Magnetic Resonance Imaging*, 2010.

[16] D. Rousseau, A. Delahaies, and F. Chapeau-Blondeau, "Structural similarity measure to assess improvement by noise in nonlinear image transmission," *IEEE Signal Processing Letters*, vol. 17, pp. 36–39, 2010.

[17] X. Bohou, J. Zhong-Ping, W. Xingxing, and D. Repperger, "Theoretical analysis of image processing using parameter-tuning stochastic resonance technique," in *Proceedings of American Control Conference*, 2007, pp. 1747–1752.

[18] ——, "Nonlinear bistable stochastic resonance filters for image processing," in *Proceedings of IEEE International Conference on Acoustics, Speech and Signal Processing*, vol. 1, 2007, pp. 717–720.

[19] P. Renbin, C. Hao, P. Varshney, and J. Michels, "Stochastic resonance: An approach for enhanced medical image processing," in *Proceedings of Life Science Systems and Applications Workshop*, 2007, pp. 253–256.

[20] Y. Yang, Z. Jiang, B. Xu, and D. Repperger, "Investigation of 2-d psr and applications in nonlinear image processing," *J. Physics A: Math. Theor.*, 2009.

[21] A. Histace and D. Rousseau, "Constructive action of noise for scalar image restoration," *Electronics Letters*, vol. 42, no. 7, pp. 393–395, 2006.

[22] ——, "Noise-enhanced anisotropic diffusion for image scalar restoration," in *Proceedings of the fifth PSIP congress (Physics in Signal and Image Processing*, 2007.

[23] P. Perona and J. Malik, "Scale-space and edge detection using anistropic diffusion," *IEEE Transcations on Pattern Analysis and Machine Intelligence*, vol. 12, no. 7, pp. 629–639, 1990.

[24] F. Vaudelle, J. Gazengel, G. Rivoire, X. Godivier, and F. Chapeau-blondeau, "Stochastic resonance and noise-enhanced transmission of spatial signals in optics: The case of scattering," *Journal of the Optical Society of America B*, vol. 13, pp. 2674–2680, 1998.

[25] L. Alvarez, F. Guichard, P. Lions, and J. Morel, "Image selective smoothing and edge detection by nonlinear diffusion (ii)," *Arch. Rationnal Mech. Anal.*, vol. 29, no. 3, pp. 845–866, 1992.

[26] F. Catté, T. Coll, P. Lions, and J. Morel, "Image selective smoothing and edge detection by nonlinear diffusion," *SIAM Journal of Applied Mathematics*, vol. 29, no. 1, pp. 182–193, 1992.

[27] S. Geman and G. Reynolds, "Constrained restoration and the recovery of discontinuities," *IEEE Transactions on Pattern Analysis and Machine Intelligence*, vol. 14, no. 3, pp. 367–383, 1992.

[28] M. Nitzberg and T. Shiota, "Nonlinear image filtering with edge and corner enhancement," *IEEE Transactions on Pattern Analysis and Machine Intelligence*, vol. 14, no. 8, pp. 826–833, 1992.

[29] R. Whitaker and S. Pizer, "A multi-scale approac to nonuniform diffusion," *CVGIP:Image Understanding*, vol. 57, no. 1, pp. 99–110, 1993.

[30] J. Weickert, "Multiscale texture enhancement," in *Computer Analysis of Images and Patterns*, 1995, pp. 230–237.

[31] R. Deriche and O. Faugeras, "Les edp en traitements des images et visions par ordinateur," *Traitement du Signal*, vol. 13, no. 6, pp. 551–578, 1996.

[32] J. Weickert, *Anisotropic Diffusion in image processing*. Stuttgart: Teubner-Verlag, 1998.

[33] R. Terebes, O. Lavialle, P. Baylou, and M. Borda, "Mixed anisotropic diffusion," in *Proceedings of the 16th International Conference on Pattern Recognition*, vol. 3, 2002, pp. 1051–4651.

[34] D. Tshumperlé and R. Deriche, "Diffusion PDEs on vector-valued images," *Signal Processing Magazine, IEEE*, vol. 19, no. 5, pp. 16–25, September 2002.

[35] D. Tschumperle and R. Deriche, "Vector-valued image regularization with pde's: A common framework for different applications." *IEEE Transactions on Pattern Analysis and Machine Intelligence*, vol. 27, pp. 506–517, 2005.

[36] A. Histace and D. Rousseau, "Noise-enhanced Nonlinear PDE for Edge Restoration in Scalar Images," in *Proceedings of SOCPAR 2010 SOft Computing and PAttern Recognition*, IEEE, Ed., Cergy France, 12 2010, pp. 458–461. [Online]. Available: http://hal.archives-ouvertes.fr/hal-00531098/en/

Author Biographies

Aymeric Histace was born in 1977 in Lyon, France. He received the Master degree in Signals/Images for Computer Aided Diagnosis in 2001 (University of Angers, France). He received, in 2004, the Ph.D degree in signal and image processing at the Laboratoire d'Ingénierie des Systèmes Automatisés (LISA), University d'Angers, France. He is since 2006, an associate professor in signal and image processing with application to life sciences (mainly Computer Aided Diagnosis) at the University of Cergy-Pontoise, Cergy, France with ETIS laboratory (UMR CNRS 8051).

David Rousseau was born in 1973 in France. He received the Master degree in acoustics and signal processing from the Institut de Recherche Co-ordination Acoustique et Musique (IRCAM), Paris, France in 1996. He received, in 2004, the Ph.D. degree in nonlinear signal processing and stochastic resonance at the Laboratoire d'Ingénierie des Systèmes Automatisés (LISA), University d'Angers, France. He is, since 2011, a full Professor in physics and information sciences with application to life sciences at Université de Lyon, France with the Laboratoire CREATIS.